Cellular Internalization and *in Vivo* Tracking of Thermosensitive Luminescent Micelles Based on Luminescent Lanthanide Chelate

Yong-Yong Li,[†] Han Cheng,[†] Zhi-Guo Zhang,[†] Chang Wang,[‡] Jing-Ling Zhu,[†] Yong Liang,[§] Ke-Li Zhang,[†] Si-Xue Cheng,[†] Xian-Zheng Zhang,[†,*] and Ren-Xi Zhuo[†]

[†]Key Laboratory of Biomedical Polymers of Ministry of Education & Department of Chemistry, Wuhan University, Wuhan 430072, People's Republic of China, [‡]Key Laboratory of Subtropical Agriculture & Environment of Ministry of Agriculture, Huazhong Agricultural University, Wuhan 430070, People's Republic of China, and [§]Department of Biology, School of Life Science and Medicine, Jianghan University, Wuhan 430056, People's Republic of China

ABSTRACT An amphiphilic tris(dibenzoylmethanato)europium(III) ($Eu(DBM)_3$) coordinated P(MMA-*co*-EIPPMMA)-*co*-P(NIPAAm-*co*-NDAPM) copolymer was synthesized, which exhibited good biocompatibility and emitted strong red luminescence (MMA, methyl methacrylate; EIPPMMA, 4-(1-ethyl-1*H*-imidazo[4,5-*f*][1,10]phenanthrolin-2-yl)phenyl methacrylate; NIPAAm, *N*-isopropylacrylamide; NDAPM, (*N*-(3-dimethylamino)propyl)methacrylamide). The copolymer could self-assemble into micelles of size around 260 nm, and the micelles were thermosensitive at around body temperature. The drug-loaded micelles showed thermosensitive controlled drug release, and the paclitaxel loaded micelles were capable of being internalized into the tumor cells (A549) and exhibited obvious inhibition to the growth of A549 cells. Importantly, *in vivo* study showed the self-assembled micelles of $Eu(DBM)_3$ coordinated P(MMA-*co*-EIPPMMA)-*co*-P(NIPAAm-*co*-NDAPM) copolymer uptaken by the larvae of zebrafish could be easily tracked and be eliminated from the body within several days.

KEYWORDS: cell internalization · *in vivo* tracking · luminescence · self-assembled micelle · controlled release

Polymeric micelles are nanosized particles with a typical core–shell structure where the core can solubilize the hydrophobic drug and the corona stabilizes the interface between the core and the outside medium.[1] Since the use of block polymer micelles as drug-carrying vehicles was proposed in 1980s, micellar drug delivery systems (DDSs), which are aimed to deliver drugs at predetermined rates and predefined periods of time, have attracted increasing research attention.[1–9] Since to know the fate of the micelles and to track the micelles in biological systems are very important for further applications of micellar DDSs, fluorescent labels on micelles have received increasing interest for biological imaging, labeling, and sensing in a variety of biological investigations especially for *in vivo* studies.

The fluorescent label approaches are divided into two main catalogues: fluorescent dye or quantum dot encapsulated micelles,[10,11] and micelles with chemically conjugated fluorescent dyes.[12–14] For example, Disher reported the application of the fluorescent probe in the study on the degradation of PEG-*b*-PCL micelles through labeling the hydrophobic segments of the micelles.[15] To date, there are many fluorescent dyes used in biological environments, and using fluorescent-labeled micelles for biological imaging has attracted great research interest. However, the fluorescent dyes generally have broad emission spectra, which usually have interference with the excitation spectra or the background of the biological systems. Recently, the near-infrared (NIR) fluorophores were frequently used in biological imaging,[16] but conventional NIR fluorophores were usually directly exposed *in vivo* due to their water solubility which may damage the organs due to intracellular accumulation. Besides, although quantum dot fluorophores were also frequently used in biological imaging, quantum dots generally suffer from cytotoxicity and leakage into biological environments.

Very recently, luminescent lanthanide chelates with unique properties such as high color purity and insensitivity to environmental quenching were found to have great potential to substitute the conventional dyes in bioimaging and biolabeling applications.[17] Of those, Eu(III)-based coordination complexes are a top priority due to their red emission having almost no interference with the background of the

*Address correspondence to xzzhang@whu.edu.cn.

Received for review May 15, 2007 and accepted December 13, 2007.

Published online January 22, 2008.
10.1021/nn700145v CCC: $40.75

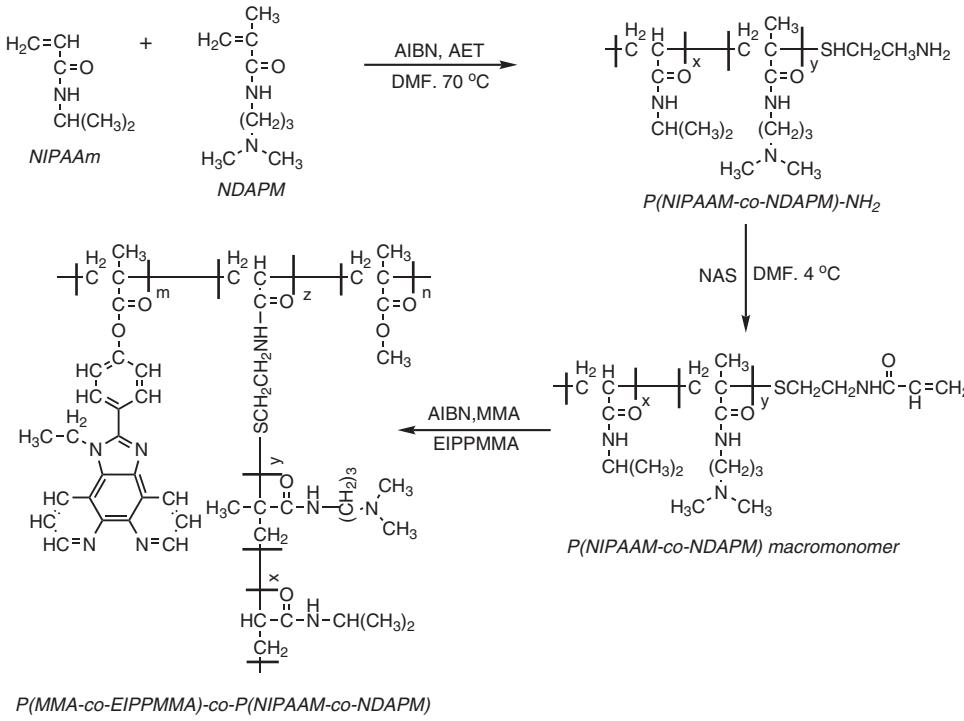

Scheme 1. Synthesis Procedure of P(MMA-*co*-EIPPMMA)-*co*-P(NIPAAm-*co*-NDAPM) Copolymer

biological systems.[18] Vandevyver *et al.* reported nontoxic lanthanide bimetallic triple-stranded helicates as the potential cellular imaging probes.[19] Generally, Eu(III)-based coordination complexes were excited with UV light. To overcome the limitations of the UV light excitation, the two-photon excitation−excitation energy transfer (TPE-EET) technology provides a new way for less-harmful and deep-penetrating bioimaging applications.[17]

In this paper, we prepared a new type of multifunctional tris(dibenzoylmethanato)europium(III) ($Eu(DBM)_3$) coordinated polymeric micelles, which exhibited a thermosensitive-controlled drug release behavior. Importantly, we developed the method of cell tracking based on the properties of luminescent lanthanide chelates, which may find great potential in drug delivery and biological imaging.

RESULTS AND DISCUSSION

The polymer synthesis is illustrated in Scheme 1. The chemical structure of the copolymer P(MMA-*co*-EIPPMMA)-*co*-P(NIPAAm-*co*-NDAPM) was characterized by ^{1}H NMR (Figure 1, panel a) and FT-IR (Figure 2). The ^{1}H NMR spectrum of the polymer in $CDCl_3$ exhibited a signal at δ 3.99 ppm which was assigned to the hydrogen of N−C*H*< in isopropylacrylamide repeating units and a peak at δ 3.60 ppm which was assigned to the hydrogen of –OCH_3 in MMA units, respectively. As shown in the FT-IR spectra in Figure 2, for P(MMA-*co*-EIPPMMA)-*co*-P(NIPAAm-*co*-NDAPM) copolymer, the absorbance of amide carbonyl group in P(NIPAAm-*co*-NDAPM)−NH_2 occurred at 1650 cm^{-1} and the bending frequency of amide N−H appeared at 1550 cm^{-1}. Besides, there was a peak at 1720 cm^{-1} due to the stretching vibration of C═O in −$COOCH_3$, which confirmed the structure of the copolymer. It was found that most probably only one P(NIPAAm-*co*-NDAPM) macromonomer was impregnated in each polymer chain from the results of GPC data (P(NIPAAm-*co*-NDAPM), M_n 20,100, PDI 1.53 and P(MMA-*co*-EIPPMMA)-*co*-P(NIPAAm-*co*-NDAPM), M_n 31,100, PDI 1.56).

The copolymer was endowed with luminescent property by coordinating with $Eu(DBM)_3$ in ethanol. The weight ratio of Eu was determined by the method of inductively coupled plasma atomic emission spec-

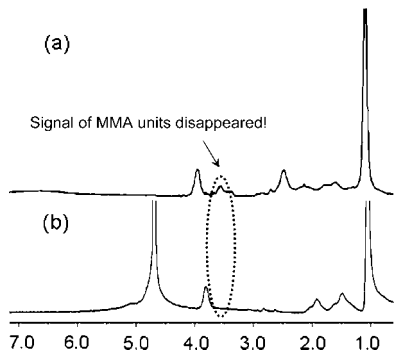

Figure 1. ^{1}H NMR spectra of P(MMA-*co*-EIPPMMA)-*co*-P(NIPAAm-*co*-NDAPM) copolymer in $CDCl_3$ (a) and its freeze-dried micelles in D_2O (b).

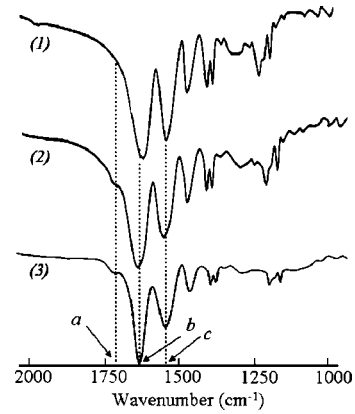

Figure 2. FT-IR spectra of (1) P(NIPAAm-*co*-NDAPM)-NH_2, (2) P(MMA-*co*-EIPPMMA)-*co*-P(NIPAAm-*co*-NDAPM) copolymer, and (3) P(MMA-*co*-EIPPMMA)-*co*-P(NIPAAm-*co*-NDAPM) micelles: a, 1720; b, 1650; c, 1550 cm^{-1}).

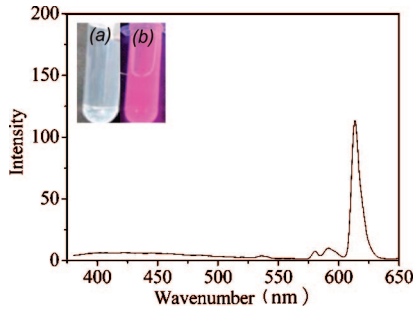

Figure 3. The emission spectrum of the Eu(DBM)$_3$ coordinated copolymer excited at 330 nm. (The insert shows the optical images of the copolymer in water before (a) and after (b) the excitation under UV light.)

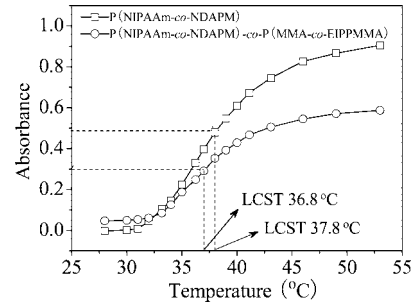

Figure 4. Thermosensitive behavior of P(NIPAAm-*co*-NDAPM) copolymer and self-assembled P(MMA-*co*-EIPPMMA)-*co*-P(NIPAAm-*co*-NDAPM) micelles upon temperature changes. (LCST was determined by absorbance at 500 nm. Copolymer concentration was 250 mg/L.)

troscopy (ICP-AES), and it was found to be 0.16%. The emission spectrum of the Eu(DBM)$_3$ coordinated P(MMA-*co*-EIPPMMA)-*co*-P(NIPAAm-*co*-NDAPM) showed there was a strong sharp peak at around 620 nm as shown in Figure 3, indicating that the copolymer solution could emit red fluorescence. The spectrum of copolymer consisted of two groups of emission peaks. The first group of weak peaks was in the region of 400–550 nm. This broad emission band was associated with the $\pi^* \rightarrow \pi$ transition of the phen moieties of the copolymer. Besides, the emission band in the red region consisted of three sharp peaks, which originated from the transitions between the 4f states of the europium ion in the copolymers. Among the organic ligands of europium complex, β-diketones play the important role due to the "antenna" effect. However, the unsaturated Eu(III) complexes, such as Eu(DBM)$_3$, tend to trap H_2O molecules to form saturated complexes and thus are harmful to luminescence. Neutral ligands such as phen not only can saturate the coordination number of the Eu(III) ion but also can improve the stability and luminescence efficiency. Since the emission from rare earth ions originates from transitions between the f levels that are well protected from environmental perturbations by the filled 5S2 and 5P6 orbitals, all of the resulting emission spectra of the europium complex exhibit sharp spectral bands corresponding to 5DJ−7FJ transitions and the profiles are identical to each other.

In our study, the coordinated polymer solution was deposited for 1 month to examine the stability of the coordinated polymer solution. It was found that the fluorescence spectra of the coordinated P(MMA-*co*-EIPPMMA)-*co*-P(NIPAAm-*co*-NDAPM) did not change, indicating that the coordinated polymer solution was stable in water. Since few organisms emit red fluorescence, the strong and pure red fluorescence and the high span (290 nm) between excitation wavelength (330 nm) and emission wavelength (620 nm) of our copolymer could minimize the interference from the background of biological systems and eliminate the disturbance of excitation spectra. Schematic illustration of luminescent P(MMA-*co*-EIPPMMA)-*co*-P(NIPAAm-*co*-NDAPM) copolymer is shown in Scheme 2.

The prepared P(MMA-*co*-EIPPMMA)-*co*-P(NIPAAm-*co*-NDAPM) copolymer had an amphiphilic nature. The hydrophobic segment was composed of MMA and EIPPMMA units, and EIPPMMA units were incorporated to coordinate Eu(III) for the fluorescence labeling. The hydrophilic segment, P(NIPAAm-*co*-NDAPM) chain, was temperature sensitive and the NDAPM units were used to adjust the lower critical solution temperature (LCST). It is well-known that the LCST of PNIPAAm is around 32−33 °C which is lower than the body temperature (37 °C). Through introducing hydrophilic monomer, *i.e.*, NDAPM units into the PNIPAAm chain, the LCST of the

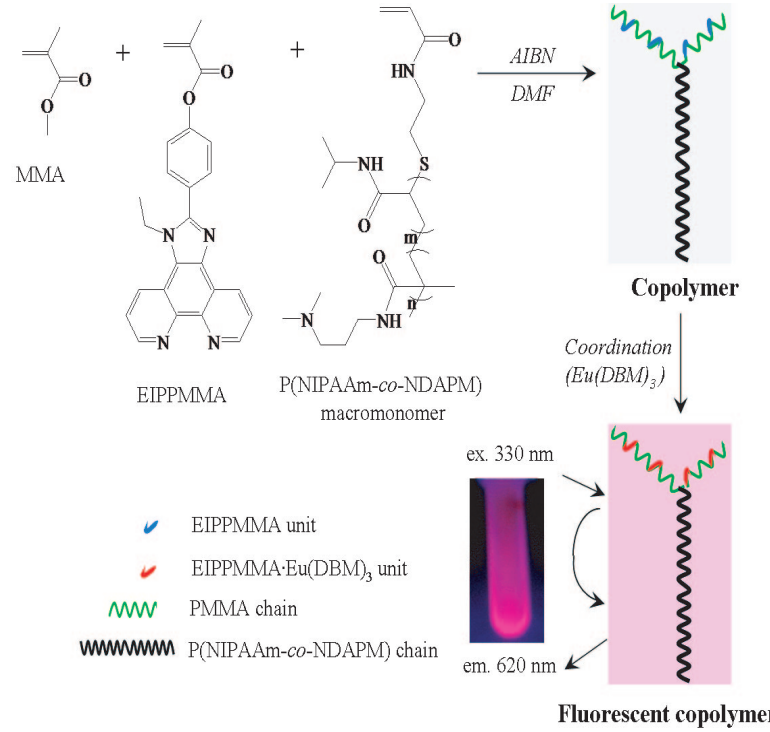

Scheme 2. Schematic Illustration of Luminescent Eu(DBM)$_3$ Coordinated P(MMA-*co*-EIPPMMA)-*co*-P(NIPAAm-*co*-NDAPM) Copolymer

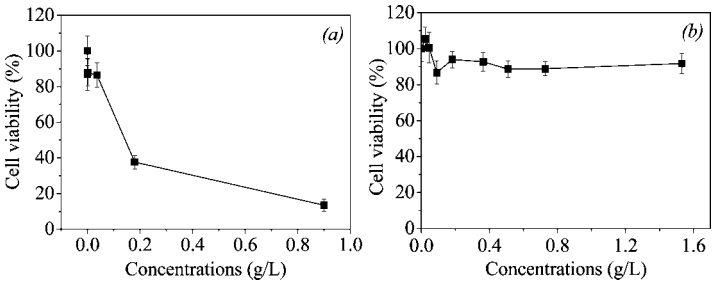

Figure 5. Cell viability of human vein endothelial cells (ECV304) incubated with the P(MMA-*co*-EIPPMMA)-*co*-P(NIPAAm-*co*-NDAPM) polymer (a) and its Eu(DBM)$_3$ coordinated copolymer (b) with different concentrations for 48 h.

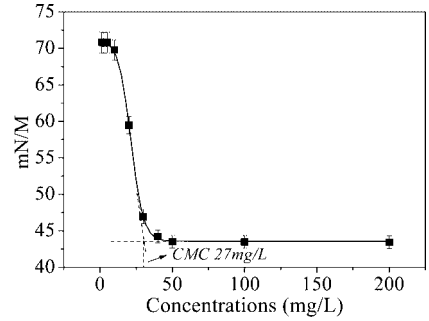

Figure 7. cmc determined from the curve of surface tension as a function of P(MMA-*co*-EIPPMMA)-*co*-P(NIPAAm-*co*-NDAPM) polymer concentration.

resultant copolymer could be tuned to body temperature for a better biological application. It was found that the resulting P(NIPAAm-*co*-NDAPM) exhibited a LCST at 37.8 °C and P(MMA-*co*-EIPPMMA)-*co*-P(NIPAAm-*co*-NDAPM) copolymer exhibited a LCST at 36.8 °C as exhibited in Figure 4. Figure 4 also shows that the LCST of P(MMA-*co*-EIPPMMA)-*co*-P(NIPAAm-*co*-NDAPM) (36.8 °C) was slightly lower than that of P(NIPAAm-*co*-NDAPM) (37.8 °C), which was attributed to the presence of hydrophobic segment of P(MMA-*co*-EIPPMMA).

The cytotoxicity study on an endothelial cell line (ECV304) was carried out to investigate the preliminary biocompatibility of resulting P(MMA-*co*-EIPPMMA)-*co*-P(NIPAAm-*co*-NDAPM) polymer and its Eu(DBM)$_3$ coordinated polymer. As shown in Figure 5, the polymer before coordination with Eu(DBM)$_3$ exhibits apparent inhibition effect on ECV304 cells when the concentration is above 30 mg/L. However, the polymer after coordinating with Eu(DBM)$_3$ does not exhibit an apparent inhibition effect on ECV304 cells even at concentrations up to 1600 mg/L. The difference in cytotoxicity was ascribed to the coordinating capacity of pyridine units in the EIPPMMA units.

As we know, nonlinear asymmetric block copolymers exhibit different micellization behaviors compared to the traditional amphiphilic copolymers.[20,21] For example, they have very different core−corona interfaces. In our previous study, it was found that the micelles self-assembled from the nonlinear asymmetric block copolymers had higher drug-loading efficiency.

To determine the critical micellar concentration (cmc) of our copolymer, pyrene was used as a hydrophobic fluorescent probe because pyrene is preferentially solubilized in the interior hydrophobic regions of these aggregates. The fluorescent intensity of pyrene under excitation is polarity-depending and it would be greatly improved when it is transferred from polar environment to nonpolar environments. From the plot of fluorescence intensity *versus* copolymer concentration in Figure 6, an abrupt increase in the total fluorescent intensity was observed with increasing copolymer concentrations, indicating formation of micelles and the transfer of pyrene into the hydrophobic core of micelles. This concentration was defined as the cmc and the cmc value of the P(MMA-*co*-EIPPMMA)-*co*-P(NIPAAm-*co*-NDAPM) copolymer was 20 mg/L.

It is well-known that surface tension would greatly decrease if the amphiphilic polymers self-assemble in the interface between water and atmosphere. When the interface is completely transformed to hydrophobic, the amphiphilic polymers will start to self-assemble into micelles in solution, where the surface tension of the solution will achieve a minimum value. The surface tension as a function of copolymer concentrations is also shown in Figure 7. The cmc value of the P(MMA-*co*-EIPPMMA)-*co*-P(NIPAAm-*co*-NDAPM) copolymer determined by surface tension measurement was around 27 mg/L.

The micelle morphology was observed by atomic force microscopy (AFM) at room temperature. The AFM micropicture in Figure 8, panel a, shows that the dried self-assembled micelles are well-dispersed as individual spherical-shaped nanoparticles with a mean diameter of 130 ± 50 nm. The size of the micelles in aqueous solution was further analyzed by a particle size analyzer, and it was found that the size of micelles was around 260 nm as shown in Figure 8, panel b. The smaller diameter from AFM study may be due to the collapse of the free segments of hydrophilic chains as well as the dehydration of the polymer chains.

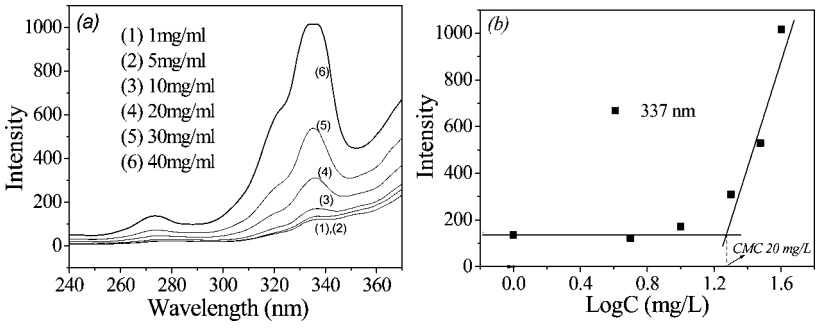

Figure 6. (a) The fluorescence–excitation spectra of pyrene with different P(MMA-*co*-EIPPMMA)-*co*-P(NIPAAm-*co*-NDAPM) polymer concentrations. (b) cmc determined from the curve of intensity as a function of log *C*.

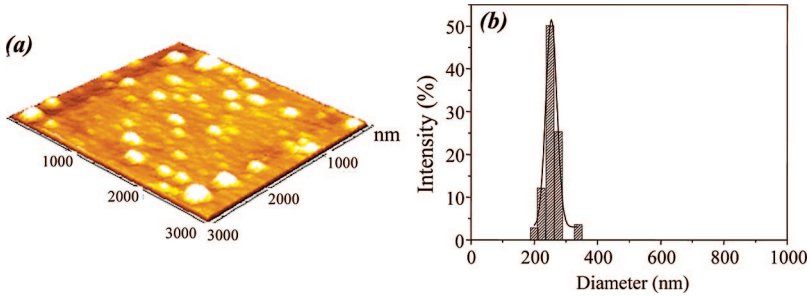

Figure 8. AFM micropicture (a) and size distribution (b) of the micelles self-assembled from the P(MMA-*co*-EIPPMMA)-*co*-P(NIPAAm-*co*-NDAPM) polymer in water. (The concentration of the copolymer was 250 mg/L.)

The micellar structure was further confirmed by ^{1}H NMR and FT-IR. The freeze-dried P(MMA-*co*-EIPPMMA)-*co*-P(NIPAAm-*co*-NDAPM) micelles were used for ^{1}H NMR (Figure 1) and FT-IR characterizations (Figure 2, spectrum 3). Compared with the ^{1}H NMR of P(MMA-*co*-EIPPMMA)-*co*-P(NIPAAm-*co*-NDAPM) polymer in $CDCl_3$ (Figure 1, panel a) and D_2O (Figure 1, panel b), the peak of MMA at 3.60 ppm disappeared in D_2O. With respect to the FT-IR, it was found that the relative absorbance of C═O in the ester linkage (Figure 2, spectrum 3) was weaker than the one in the spectrum of P(MMA-*co*-EIPPMMA)-*co*-P(NIPAAm-*co*-NDAPM) copolymer (Figure 2, spectrum 2), which is attributed to the fact that the copolymer formed a core–shell micellar structure with the isolated hydrophobic inner core and hydrophilic outer shell.

The controlled drug release from P(MMA-*co*-EIPPMMA)-*co*-P(NIPAAm-*co*-NDAPM) micelles was examined *in vitro*, and the release data are presented in Figure 9, panel a. Prednisone acetate is an anti-inflammatory drug, and paclitaxel is an anticancer drug used in clinical practice and exhibits strong cure effects against a variety of cancer types. Both drugs have a very low solubility in water. In order to improve the solubility and enhance the therapeutic efficiency, hydrophobic drugs were entrapped into the hydrophobic cores of the micelles. The primary advantage of its encapsulation into the micelles is the enhanced solubility. It was found that both drugs loaded in micelles showed a similar controlled release behavior. The drug release profiles revealed drastic changes with the temperature alteration around the LCST. When the temperature was 16 °C (below the LCST), the drug release rates were relatively slow. When the release temperature was 38 °C (above the LCST), the P(NIPAAm-*co*-NDAPM) shells became hydrophobic, which led to the deformation of micellar structures. As a result, the drug release was much accelerated due to the temperature-induced structure change of the micelles. A potential application of such a themosensitive drug releasing property is that we could adjust the drug release rate as well as the therapy effect through temperature alteration, for example, in thermotherapy for some particular cases.

The cure efficacy of paclitaxel-loaded micelles on the inhibition of the growth of A549 cells was further investigated. The A549 cells were incubated for 48 h with the paclitaxel-loaded micelles and the experimental result is presented in Figure 9, panel b. After treatment with drug-loaded micelles, the A549 cells exhibited obviously lower viability compared with the cells treated with the blank micelles. Such results indicated that the paclitaxel-loading micelles exhibited obvious inhibition to the growth of A549 cells. The content of paclitaxel loaded in the micelles was also figured out through the entrapment efficiency (15.6%), and we further compared the cell viability of the free paclitaxel to that of drugs loaded in micelles with different concentrations (Figure 9, panel c). The highest concentration of the free paclitaxel was the saturated concentration of paclitaxel (4.7 mg/L) due to its poor solubility in aqueous solution. The IC50 of the drug-loaded micelles was around 20 mg/L, corresponding to 3 mg/L of the loaded paclitaxel, which was a little higher than the IC50 of pure paclitaxel (2 mg/L). More drugs could be loaded and thereafter delivered to tumor cells by the use of micelles. In addition, the paclitaxel in the micelles was release gradually, which greatly reduced the cytotoxicity of paclitaxel.

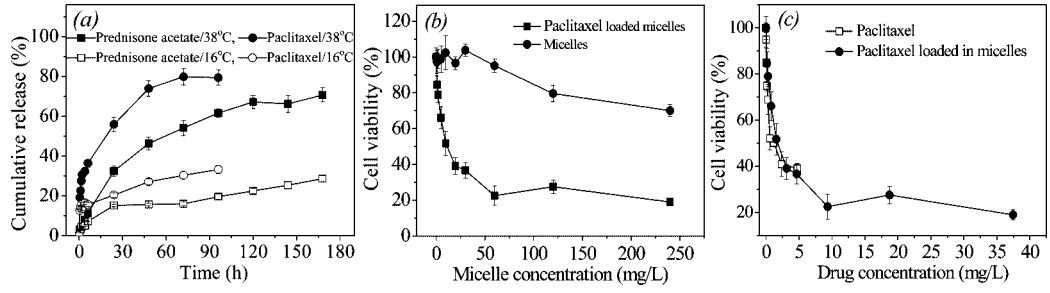

Figure 9. a) Drug release behavior of thermosensitive P(MMA-*co*-EIPPMMA)-*co*-P(NIPAAm-*co*-NDAPM) micelles loaded with prednisone acetate or paclitaxel at 16 and 38 °C respectively. b) A549 cell viability in the presence of micelles or paclitaxel loaded micelles with different concentrations. c) A549 cell viability in the presence of free paclitaxel and paclitaxel loaded in micelles with different concentrations.

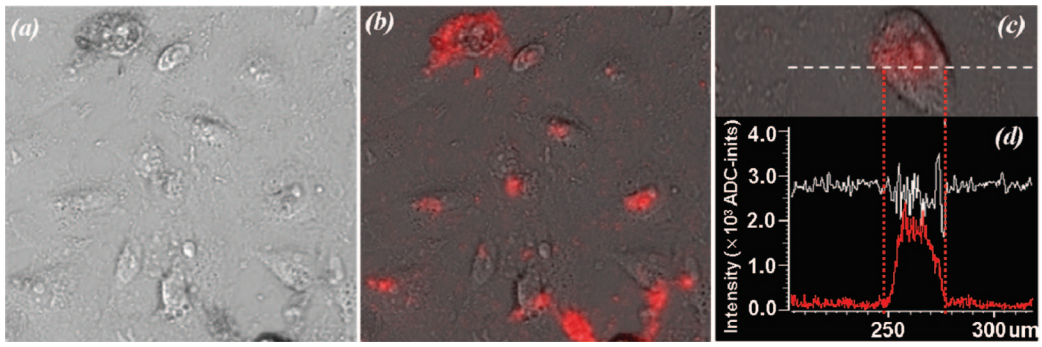

Figure 10. Images of A549 cells with blank micelles: a) under bright field; b) under bright field with excitation at 405 nm; c) one A549 cell with a higher magnification; d) fluorescent intensity (red curve) outside and inside the A549 cell.

To examine whether the micelles could enter the tumor cells (A549 cell line) for potential antitumor therapy, the cellular internalization of drug-loaded micelles was investigated. After 24 h of incubation with the micelles, the A549 cells were observed by a laser scanning confocal microscope and the result is demonstrated in Figure 10. It was found that the micelles could be internalized into the A549 cells because the fluorescent intensity increased suddenly inside an A549 cell (Figure 10, panel d).

To investigate the biocompatibility as well as the fluorescent property of self-assembled micelles after entering the bodies of organisms, zebrafish was chosen as a model organism for *in vivo* study. Zebrafish, with a high-resolution genetic map, a full physical map, and physiological and pharmacological similarities to humans, has been widely used in toxicity test of biomedical materials, genetics, and auxanology as a model organism.[22–24] In addition, due to their tiny bodies, transparent offspring, and high propagation ability, the micelles can be easily tracked in the living zebrafish, and the *in vivo* assays are high-throughput and low-cost. In the current study, the *in vivo* test showed that the micelles had good biocompatibility. After 6 days' exposure to the micelle suspension with a copolymer concentration of 100 mg/L, the viability of the test group was 93.4%, while that of the control group was 96.7% ($n = 30$). No abnormality in two groups was found. Before the zebrafish hatched, it was found that the micelles just stuck on the membrane (Figure 11, panel B_i) compared with the full shot of the embryos (Figure 11, panel A_i). However, after hatching at the fifth and sixth day, it was found that micelles existed inside the bodies of the fish (Figure 11, panel B_{ii}) compared with the full shot of the whole fish (Figure 11, panel A_{ii}). It was speculated that the micelles could be uptaken by the larvae. After the larvae were transferred into the fresh water, the fluorescence in larvae ($n = 24$) was almost faded at the third day (Figure 11, panel B_{iii}) due to excretion. The results showed that micelles did not exhibit toxic effects on the embryos and larvae, which was consistent with *in vitro* cytotoxicity study on ECV304 cells. More importantly, the micelles could be eliminated from the body within several days, which is comparable with the drug release time of conventional drug carriers. That means the micelles could be removed from the body once the controlled drug release is completed.

CONCLUSIONS

In summary, a novel amphiphilic thermosensitivity P(MMA-*co*-EIPPMMA)-*co*-P(NIPAAm-*co*-NDAPM) copoly-

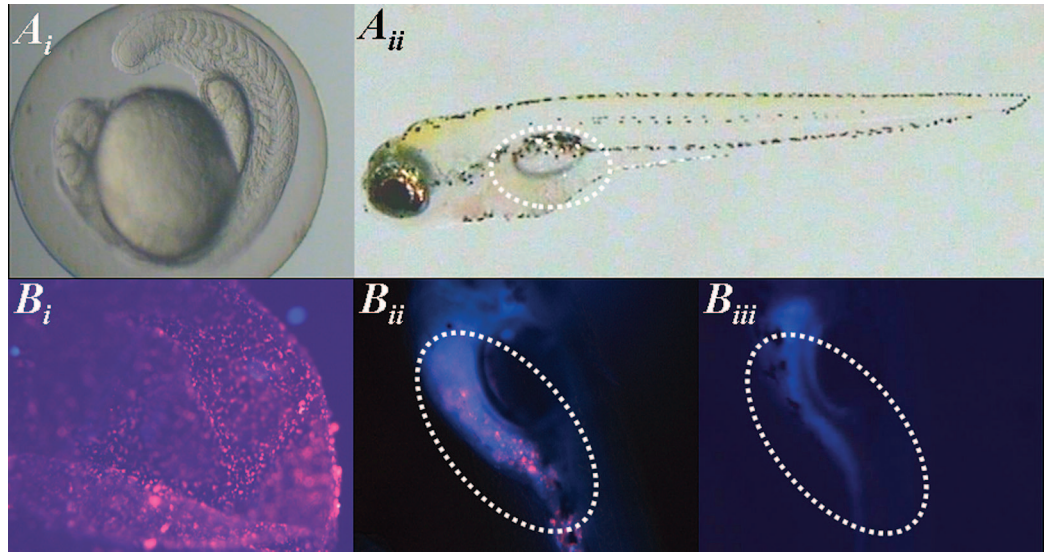

Figure 11. Images of zebrafish embryo (A_i), a full body shot of a fish (A_{ii}), zebrafish embryo exposure to micelles (B_i), and larva after treatment with micelles for 6 days (B_{ii}) and then with fresh water for 3 days (B_{iii}). The images of B_i, B_{ii}, and B_{iii} were obtained by excitation under UV light with a blue background.

mer was synthesized. After coordination with tris(dibenzoylmethanato)europium(III) ($Eu(DBM)_3$), the copolymer exhibited good biocompatibility and fluorescence property. The $Eu(DBM)_3$ coordinated copolymer could emit red luminescence (620 nm) when excited at 330 nm, and the high span (as high as 290 nm) between the excitation wavelength and emission wavelength is favorable to avoid the disturbance of excitation light and background. *In vivo* study showed the self-assembled micelles uptaken by the larvae of zebrafish could be easily tracked and be eliminated from the body within several days. The drug-loaded micelles exhibited a thermosensitive controlled release behavior and were capable of being internalized into the tumor cells (A549) and exhibited obvious inhibition to the growth of A549.

EXPERIMENTAL SECTION

Materials. 4-(1-Ethyl-1*H*-imidazo[4,5-*f*][1,10]phenanthrolin-2-yl)phenyl methacrylate (EIPPMMA) and tris(dibenzoylmethanato)europium(III) ($Eu(DBM)_3$) were synthesized in the laboratory.[25] *N*-Acroyloxysuccinimide (NAS) was synthesized according to the reported procedure.[26] *N*-Isopropylacrylamide (NIPAAm), methyl methacrylate, and 2-aminoethanethiol hydrochloride (AET · HCl) were purchased from ACROS and used as received. *N,N′*-Azobisisobutyronitrile (AIBN) provided by Shanghai Chemical Reagent Co. (People's Republic of China) was used after recrystallization with 95% ethanol. *N*-(3-(Dimethylamino)propyl)methacrylamide (NDAPM) was purchased from Japan Mark lot. DMEM and RPMI-1640 were obtained from GIBCO Invitrogen Corp. All other reagents were used without further purification.

Synthesis of Amino-Terminated P(NIPAAm-*co*-NDAPM). P(NIPAAm-*co*-NDAPM) with a terminal amino group was synthesized by free-radical polymerization of NIPAAm (5.49 g, 50 mmol), NDAPM (50 μL, 0.5 mmol) in DMF (27.5 mL) using AIBN (11 mg, 0.07 mmol), and AET · HCl (90 mg, 0.8 mmol) as an initiator and chain transfer reagent, respectively.[7] After all the reactants were well-mixed, the solution was degassed by bubbling with nitrogen for 30 min. Then the polymerization reaction was performed at 70 °C under a N_2 atmosphere for 24 h. P(NIPAAm-*co*-NDAPM)$-NH_2$ was obtained by precipitating the reaction solution into diethyl ether. The product was purified by repeated precipitation in diethyl ether from ethanol and then dried in vacuum to obtain amino-terminated P(NIPAAm-*co*-NDAPM) with a yield of 81.1%.

Synthesis of P(NIPAAm-*co*-NDAPM) Macromonomer. P(NIPAAm-*co*-NDAPM) macromonomer was synthesized through an amide condensation reaction between amino groups in P(NIPAAm-*co*-NDAPM)$-NH_2$ (0.70 g, 0.035 mmol) and NAS (0.17 g, 1 mmol) in DMF (6 mL) at 4 °C for 2 days. Then the reaction was performed at 40 °C under a N_2 atmosphere for 24 h. The obtained product was purified by repeated precipitation in diethyl ether from ethanol and then dried in vacuum to obtain P(NIPAAm-*co*-NDAPM) macromonomer with a yield of 94.6%.

Synthesis of P(MMA-*co*-EIPPMMA)-*co*-P(NIPAAm-*co*-NDAPM). P(NIPAAm-*co*-NDAPM) macromonomer (0.35 g, 0.0175 mmol), MMA (0.112 g, 1.12 mmol), EIPPMMA (24 mg, 0.06mmol), and AIBN (5 mg, 0.03 mmol) were dissolved in DMF. The solution was degassed by bubbling with nitrogen for 30 min. Then the reaction was performed at 70 °C under a N_2 atmosphere for 24 h. The obtained product was purified by repeated precipitation in diethyl ether from ethanol and then dried in vacuum to obtain P(MMA-*co*-EIPPMMA)-*co*-P(NIPAAm-*co*-NDAPM) with a yield of 96.4%. The synthesis procedure is illustrated in Scheme 1.

Preparation of $Eu(DBM)_3$ Coordinated P(MMA-*co*-EIPPMMA)-*co*-P(NIPAAm-*co*-NDAPM). P(MMA-*co*-EIPPMMA)-*co*-P(NIPAAm-*co*-NDAPM) (0.3 g) was endowed with luminescent properties by coordinating with $Eu(DBM)_3$ (20 mg) in ethanol at 60 °C. The residual $Eu(DBM)_3$ was removed by dialysis in ethanol for 7 days. Ethanol was replaced every 12 h. Then the product underwent dialysis in pure water. Finally, the polymer was freeze-dried for characterizations of cytotoxicity study, fluorescence measurements, and *in vivo* and *in vitro* tracking.

Chemical Structure Characterization. FT-IR spectra were recorded on an AVATAR 360 spectrometer and samples were pressed into potassium bromide (KBr) pellets. ^1H NMR spectra were recorded on a Varian Unity 300 MHz spectrometer and TMS was used as internal standard. Molecular weights of the polymers were determined by a gel permeation chromatographic (GPC) system equipped with a Waters 2690D separation module and a Waters 2410 refractive index detector. DMF was used as the eluent. Waters millennium module software was used to calculate molecular weight on the basis of a universal calibration curve generated by polystyrene standards of narrow molecular weight distribution. ICP-AES measurement was conducted on a 2 kW, 27 MHz ICP power source (Beijing Second Broadcast Instrument Factory, Beijing, China) and a conventional plasma torch was used.

LCST Determination. Optical absorbance of P(MMA-*co*-EIPPMMA)-*co*-P(NIPAAm-*co*-NDAPM) aqueous solution (250 mg/L) at various temperatures was measured at 500 nm with a Lambda Bio40 UV–vis spectrometer (Perkin-Elmer). The sample cell was thermostated in a refrigerated circulator bath at different temperatures from 26 to 53 °C prior to measurements. The LCST of the copolymer solution was defined as the temperature producing a half increase of the total increase in optical absorbance.

cmc Determination. Fluorescence spectra were recorded on a LS55 fluorescence spectrometer (Perkin-Elmer). Pyrene was used as a hydrophobic fluorescent probe. Aliquots of pyrene solutions (6×10^{-6} M in acetone, 1 mL) were added to containers, and acetone was allowed to evaporate. Ten milliliter aqueous polymer solutions at different concentrations were then added to the containers containing the pyrene residue. It should be noted that the concentration of pyrene in each tube was 6×10^{-7} M, which would be adequate for the cmc measurements. The solutions were kept at room temperature for 24 h to reach the equilibrated solubilization of pyrene in the aqueous phase. Emission was carried out at 390 nm, and excitation spectra were recorded ranging from 240 to 360 nm. Both excitation and emission bandwidths were 10 nm. From the pyrene excitation spectra, the intensities at 337 nm were analyzed as a function of the polymer concentrations. A cmc value was determined from the intersection of the tangent to the curve at the inflection with the horizontal tangent through the points at low concentration.

The cmc value was also determined from the surface tension as a function of copolymer concentration. The surface tension of copolymer solutions with different concentrations was measured on DataPhysics OCA30 contact angle meter and was analyzed as a function of the copolymer concentration. The cmc value was determined from the intersection of the tangent to the curve at the inflection with the horizontal tangent through the points at high concentration and the corresponding concentration was defined as cmc.

Characterization of Fluorescence Property of $Eu(DBM)_3$ Coordinated P(MMA-*co*-EIPPMMA)-*co*-P(NIPAAm-*co*-NDAPM). $Eu(DBM)_3$ coordinated P(MMA-*co*-EIPPMMA)-*co*-P(NIPAAm-*co*-NDAPM) solution with a concentration of 250 mg/L was used for fluorescence property characterization. The excitation was carried out at 330 nm, and both the excitation and emission bandwidths were 5 nm. Emission from 350 to 650 nm was detected.

Micelle Preparation and Micelle Morphology Study. Dialysis method was used to prepare the micelles. Briefly, P(MMA-*co*-EIPPMMA)-*co*-P(NIPAAm-*co*-NDAPM) copolymer (2 mg) was dissolved in 4 mL of DMF. The solution was put into a dialysis tube (MWCO: 8000–10000 g/mol) and subjected to dialysis against 1000 mL of distilled water for 24 h. Micelle morphology was observed on

a Picoscan atomic force microscope (Molecular Imaging, Tempe, AZ) in contact mode with commercial MAClever II tips (Molecular Imaging) with a spring constant of 0.95 N/m.

Drug Loading and *in Vitro* Drug Release. P(MMA-*co*-EIPPMMA)-*co*-P(NIPAAm-*co*-NDAPM) (2 mg) and a drug (2 mg of prednisone acetate or 2 mg of paclitaxel) were dissolved in 2 mL of DMF. The solution was put into a dialysis tube and subjected to dialysis against 1000 mL of distilled water for 24 h during which the water was refreshed. The dialyzate after drug loading was measured by UV spectroscopy to determine the amount of unloaded drugs. It was found that around 27.7 wt % of prednisone acetate and 15.6 wt % of paclitaxel were loaded into P(MMA-*co*-EIPPMMA)-*co*-P(NIPAAm-*co*-NDAPM) micelles.

After dialysis, the dialysis tube was directly immersed into 400 mL of distilled water with predetermined temperature. Aliquots of 3 mL were withdrawn from the solution periodically. The volume of solution was held constantly by adding 3 mL of distilled water after each sampling. The amount of prednisone acetate and paclitaxel released from micelles was measured by UV absorbance at 242 and 232 nm, respectively. The cumulative drug release was calculated as: cumulative drug release (%) = $M_t/M_0 \times 100$, where M_t is the amount of drugs released from micelles at time t and M_0 is the amount of drugs loaded in P(MMA-*co*-EIPPMMA)-*co*-P(NIPAAm-*co*-NDAPM) micelles. M_0 was estimated by subtracting the amount of unloaded drugs from the feed drug amount (2 mg).

***In Vitro* Cytotoxicity Study and Inhibition Growth of Tumor Cells.** Human vein endothelial cells (ECV304) were used for *in vitro* cytotoxicity test, and human lung adenocarcinoma cells (A549) were used to study the inhibition growth of the tumor cells treated by the drug loaded micelles. After incubation for 24 h in incubator (37 °C, 5% CO_2), the culture medium was replaced by 200 μL of RPMI-1640 (for ECV304 cells) containing micelles with particular concentrations or DMEM (for A549 cells) containing micelles or drug-loaded micelles with particular concentrations and the mixture was further incubated for 48 h. Then RPMI-1640 or DMEM with micelles was replaced by fresh RPMI-1640 or DMEM, and 20 μL of MTT solution (5 mg/mL) was added. After incubation for 4 h, 200 μL of DMSO was added and shaken at room temperature. The optical density (OD) was measured at 570 nm with a microplate reader, model 550 (BIO-RAD, USA). The cell viability was calculated by the following equation: viability = $(OD_{treated}/OD_{control}) \times 100\%$, where $OD_{control}$ was obtained in the absence of copolymer and $OD_{treated}$ was obtained in the presence of copolymer. Cellular internalization was studied by confocal laser scanning microscopy (LSM C1si Nikon, BD Laser) at 405 nm and 25 mW.

***In Vivo* Tracking of Micelles in Zebrafish Embryos and Larvae.** Fertilized eggs were obtained from natural mating of adult zebrafish (Danio rerio AB line) which were bred at the Animal Center of Jianghan University. Embryos were collected within 2 h of spawning. Newly fertilized eggs, approximately at the stage of 64 cells, were exposed to luminescent micelles (100 μg/mL) for 6 days. Ten eggs were placed in each well of a 12-well plate. During the exposure, 60% of each well was replaced by fresh solution daily. After 6 days of static exposure, the larvae were rinsed with water and maintained in aerating water for further observation; meanwhile, 90% of the water was replaced daily. Embryos and larvae were maintained at 27 ± 1 °C in a 14 h light and 10 h dark schedule. Each experiment was repeated three times. A group without the luminescent micelles was used as the control. All observations were done by an OLYMPUS CKX-31 inverted microscope. All of images were obtained using a Motic BA400 microscope with a Moticam 5000 device camera.

Acknowledgment. This work was financially supported by National Natural Science Foundation of China (50633020), National Key Basic Research Program of China (2005CB623903), and Ministry of Education of China (Cultivation Fund of Key Scientific and Technical Innovation Project 707043). We also acknowledge Professor L. Z. Meng (Wuhan University, People's Republic of China) for her helpful discussions.

REFERENCES AND NOTES

1. Gros, L.; Ringsdorf, H.; Schupp, H. Polymeric antitumor agents on a molecular and on a cellular level. *Angew. Chem., Int. Ed.* **1981**, *20*, 305–325.
2. Nasongkla, N.; Shuai, X. T.; Ai, H.; Weinberg, B. D.; Pink, J.; Boothman, D. A.; Gao, J. M. cRGD-functionalized polymer micelles for targeted doxorubicin delivery. *Angew. Chem., Int. Ed.* **2004**, *43*, 6323–6327.
3. Nobs, L.; Buchegger, F.; Gurny, R.; Allemann, E. Biodegradable nanoparticles for direct or two-step tumor immunotargeting. *Bioconjugate Chem.* **2006**, *17*, 139–145.
4. Liu, S. Y.; Armes, S. P. Polymeric surfactants for the new millennium: a ph-responsive, zwitterionic, schizophrenic diblock copolymer. *Angew. Chem., Int. Ed.* **2002**, *41*, 1413–1416.
5. Liu, X. K.; Jiang, M. Optical switching of self-assembly: micellization and micelle-hollow-sphere transition of hydrogen-bonded polymers. *Angew. Chem., Int. Ed.* **2006**, *45*, 3846–3850.
6. Nasongkla, N.; Bey, E.; Ren, J. M.; Ai, H.; Khemtong, C.; Guthi, J. S.; Chin, S. F.; Sherry, A. D.; Boothman, D. A.; Gao, J. M. Multifunctional polymeric micelles as cancer-targeted, MRI-ultrasensitive drug delivery systems. *Nano Lett.* **2006**, *6*, 2427–2430.
7. Li, Y. Y.; Zhang, X. Z.; Kim, G. C.; Cheng, H.; Cheng, S. X.; Zhuo, R. X. Thermosensitive Y-shaped micelles of poly(oleic acid-Y-N-isopropylacrylamide) for drug delivery. *Small* **2006**, *2*, 917–923.
8. Wei, H.; Zhang, X. Z.; Zhou, Y.; Cheng, S. X.; Zhuo, R. X. Self-assembled thermoresponsive micelles of poly(N-isopropylacrylamide-b-methyl methacrylate). *Biomaterials* **2006**, *27*, 2028–2034.
9. Webber, G. B.; Wanless, E. J.; Armes, S. P.; Tang, Y. Q.; Li, Y. T.; Biggs, S. Nano-anemones: stimulus-responsive copolymer-micelle surfaces. *Adv. Mater.* **2004**, *16*, 1794–1798.
10. Fan, H. Y.; Leve, E. W.; Scullin, C.; Gabaldon, J.; Tallant, D.; Bunge, S.; Boyle, T.; Wilson, M. C.; Brinker, C. J. Surfactant-assisted synthesis of water-soluble and biocompatible semiconductor quantum dot micelles. *Nano Lett.* **2005**, *5*, 645–648.
11. Maysinger, D.; Berezovska, O.; Savic, R.; Soo, P. L.; Eisenberg, A. Block copolymers modify the internalization of micelle-incorporated probes into neural cells. *Biochim. Biophys. Acta* **2001**, *1539*, 205–217.
12. Luo, L. B.; Tam, J.; Maysinger, D.; Eisenberg, A. Cellular internalization of poly(ethylene oxide)-b-poly(epsilon-caprolactone) diblock copolymer micelles. *Bioconjugate Chem.* **2002**, *13*, 1259–1265.
13. Savic, R.; Azzam, T.; Eisenberg, A.; Maysinger, D. Assessment of the integrity of poly(caprolactone)-b-poly(ethylene oxide) micelles under biological conditions: a fluorogenic-based approach. *Langmuir* **2006**, *22*, 3570–3578.
14. Savic, R.; Luo, L. B.; Eisenberg, A.; Maysinger, D. Micellar nanocontainers distribute to defined cytoplasmic organelles. *Science* **2003**, *300*, 615–618.
15. Geng, Y.; Discher, D. E. Hydrolytic degradation of poly(ethylene oxide)-block-polycaprolactone worm micelles. *J. Am. Chem. Soc.* **2005**, *127*, 12780–12781.
16. Leevy, W. M.; Gammon, S. T.; Jiang, H.; Johnson, J. R.; Maxwell, D. J.; Jackson, E. N.; Marquez, M.; Worms, D. P.; Smith, B. D. Optical imaging of bacterial infection in living mice using a fluorescent near-infrared molecular probe. *J. Am. Chem. Soc.* **2006**, *128*, 16476–16477.
17. Fu, L. M.; Wen, X. F.; Ai, X. C.; Sun, Y.; Wu, Y. S.; Zhang, J. P.; Wang, Y. Efficient two-photon-sensitized luminescence of a europium(III) complex. *Angew. Chem., Int. Ed.* **2005**, *44*, 747–750.
18. Santos, M.; Roy, B. C.; Goicoechea, H. C.; Campiglia, A. D.; Mallik, S. An investigation on the analytical potential of polymerized liposomes bound to lanthanide ions for protein analysis. *J. Am. Chem. Soc.* **2004**, *126*, 10738–10745.

19. Vandevyver, C. D. B.; Chauvin, A. S.; Comby, S.; Bunzli, J. C. G. Luminescent lanthanide bimetallic triple-stranded helicates as potential cellular imaging probes. *Chem. Commun.* **2007**, *17*, 1716–1718.
20. Sotiriou, K.; Nannou, A.; Velis, G.; Pispas, S. Micellization behavior of PS(PI)(3) miktoarm star copolymers. *Macromolecules* **2002**, *35*, 4106–4112.
21. Yun, J. P.; Faust, R.; Szilagyi, L. S.; Keki, S.; Zsuga, M. Effect of architecture on the micellar properties of amphiphilic block copolymers: comparison of AB linear diblock, A(1)A(2)B, and A(2)B heteroarm star block copolymers. *Macromolecules* **2003**, *36*, 1717–1723.
22. Kahn, P. Zebrafish hit the big time. *Science* **1994**, *264*, 904–905.
23. Thisse, C.; Zon, L. I. Development-organogenesis-heart and wood formation from the zebrafish point of view. *Science* **2002**, *295*, 457–462.
24. Lee, K. J.; Nallathamby, P. D.; Browning, L. M.; Osgood, C. J.; Xu, X. H. N. Nanoparticles in early development of zebrafish embryos. *ACS Nano* **2007**, *1*, 133–143.
25. Zhang, Z. G.; Yuan, J. B.; Tang, H. J.; Zhang, K. L. The convenient synthesis of novel ligand monomers derived from 1,10-phenanthroline. To be published.
26. Liu, F.; Tao, G. L.; Zhuo, R. X. Synthesis of thermal phase separating reactive polymers and their applications in immobilized enzymes. *Polym. J.* **1993**, *25*, 561–567.